ELLIPTICAL POLARIZATION IN ROTATIONAL MAGNETIC FIELD

Amália IVÁNYI

Department of Electromagnetic Theory
Technical University of Budapest
H–1521 Budapest, Hungary
Tel: (+36 1) 181 3198
Fax: (+36 1) 166 6806
E–mail: ivanyi@evtsz.bme.hu

Received: Nov. 1, 1994

Abstract

The two-dimensional measurements prove that the magnetic hysteresis shows different behaviour at rotational magnetic field comparing its properties to the alternating one. In this paper these phenomena are investigated from theoretical point of view. It is proved that due to the introduced anisotropy tensor the circular polarized rotational magnetic induction yields elliptical polarization for both components of the magnetization as well as for the **M**-field patterns. The non-zero value of the off-diagonal elements in the anisotropy tensor has influence on the width of the hysteresis loops. It is proved that at small amplitude of the circular polarized rotational magnetic flux both the **M**-field and the **H**-field patterns have elliptical polarization. Increasing the amplitude of the induction in the rotational field, at saturation region the **H**-field patterns have modification in the elliptical polarization.

Keywords: anisotropic magnetic material, rotational field, elliptical polarization of magnetization, polarization of H-field.

Introduction

Several two-dimensional measurements prove that specimens under rotating magnetic field show different properties, hysteresis loops and **H**-field patterns, comparing their behaviour under alternating magnetic field [1], [2]. In this paper these phenomena are investigated from theoretical point of view, and proved that the field locus curves are generated by the elliptical polarized **H**-field patterns in each direction.

In this paper the magnetic material is modelled with macroscopic parameters. For the investigation a two-dimensional model is introduced. In the alternating field the nonlinear characteristics of the material in both directions are approximated by inverse tangent functions without hysteresis. Taking into account the interaction between the magnetization in different directions an anisotropy tensor is introduced. Applying rotational magnetic field the affection of the anisotropy and the variation of the amplitude in the flux are studied, respectively.

1. Modelling the Nonlinear Characteristics

To describe the relation between the field intensity $\mathbf{H}$ and the flux density $\mathbf{B}$ in nonlinear magnetic material the 'magnetization' $\mathbf{M}$ is introduced

$$\mathbf{B} = \mu_0 \mathbf{H} + \mathbf{M}(\mathbf{H}) , \tag{1}$$

where the $\mathbf{M} = \mathbf{M}(\mathbf{H})$ characteristic is responsible for the hysteresis. In this paper the affection of the magnetic material on the induction is supposed to be much more higher comparing to the one of the free space ($\mu_0 \mathbf{H} \ll \mathbf{M}$), so it is neglected in relation (1)

$$\mathbf{B} \cong \mathbf{M}(\mathbf{M}) . \tag{2}$$

Introducing a two-dimensional vector model with x,y directions, the vectors of the field intensity $\mathbf{H}$, of the magnetization $\mathbf{M}$, and of the induction $\mathbf{B}$ have different directions. The interaction between the field components and the anisotropy of the material is formulated with the anisotropy tensor $\boldsymbol{\kappa}$

$$\begin{bmatrix} B_x \\ B_y \end{bmatrix} = \begin{bmatrix} \kappa_{11} & \kappa_{12} \\ \kappa_{21} & \kappa_{22} \end{bmatrix} \begin{bmatrix} M_x(H_x) \\ M_y(H_y) \end{bmatrix} . \tag{3}$$

In the model under alternating field the anhysteretic $\mathbf{M}(\mathbf{H})$ characteristics in both directions are approximated by inverse tangent functions with different parameters

$$M_i = M_i(H_i) = M_{oi} \tan^{-1}(H_i / H_{oi}), \quad i = x, y . \tag{4}$$

To identify the model the parameters are determined from the initial slope and from the point of the characteristic belonging to the highest amplitude of the magnetization. For the theoretical investigation the material is selected from the measured samples [3]. The measured maximum values of the x and y directed components in the magnetic field and the magnetization are

$$\begin{aligned} H_{x,\max} &= \ 400 \text{ A/m}, \quad M_{x,\max} = 1.4 \text{ T}, \\ H_{y,\max} &= 1600 \text{ A/m}, \quad M_{y,\max} = 1.4 \text{ T} . \end{aligned} \tag{5}$$

The measured initial relative permittivities are

$$\mu_{x,r,\text{init}} = 13263, \quad \mu_{y,r,\text{init}} = 2652. \tag{6}$$

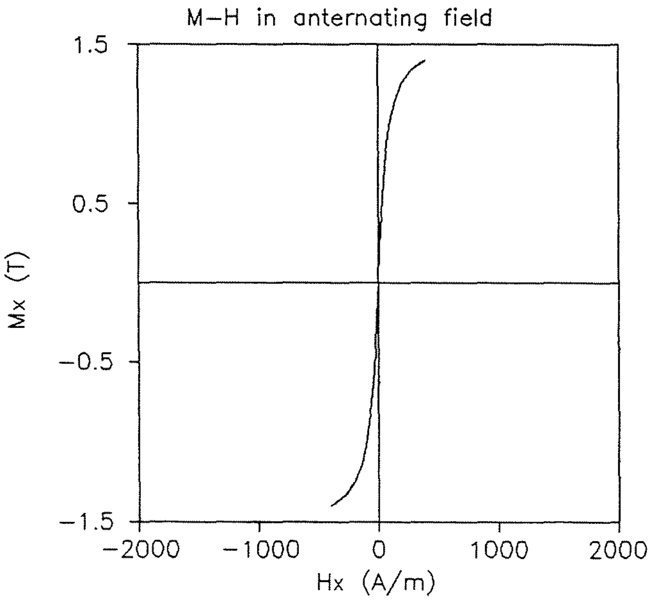

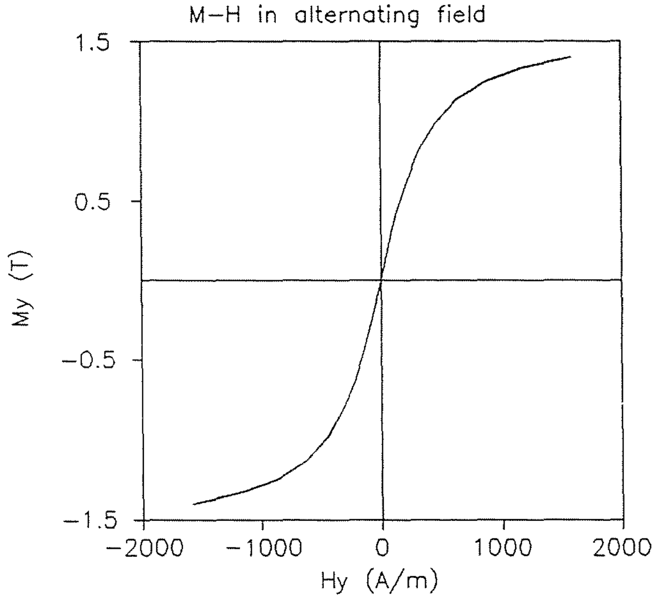

Fig. 1. The anhysteretic $M - H$ characteristics of the material in x-direction (a), and in y-direction (b) under alternating field.
(a) $M_{x,\max} = 1.4$ T, $H_{x,\max} = 400$ A/m, $\mu_{x,r,\mathrm{init}} = 13263$
(b) $M_{y,\max} = 1.4$ T, $H_{y,\max} = 1600$ A/m, $\mu_{y,r,\mathrm{init}} = 2652$

From the measured values the calculated parameters of the nonlinear characteristics are

$$M_{ox} = 0.9833 \text{ T}, \quad H_{ox} = 59.23 \text{ (A/m)},$$
$$M_{oy} = 1.0140 \text{ T}, \quad H_{oy} = 298.2 \text{ (A/m)} . \tag{7}$$

The anhysteretic behaviour of the model (4), approximating with parameters (7) in the nonlinear characteristics of the magnetic material (5)–(6), are plotted in *Fig. 1* until $B = 1.4$ T is the alternating flux.

Following the measurement techniques, an x,y directed magnetic flux density with sinusoidal variation is applied on the material

$$B_x = B_m \cos \omega t, \quad B_y = B_m \sin \omega t . \tag{8}$$

Introducing the complex formalism, the components of the applied flux result in circular polarized rotational induction

$$\mathbf{B} = B_x + jB_y = B_m e^{j\omega t} . \tag{9}$$

2. Anisotropy and Elliptical Polarization

The first examination deals with the relation between the anisotropy tensor and the rotational magnetic flux density. From the inverse of (3) the magnetization vector as well as its components can be superposed from clockwise and anti-clockwise rotating flux vectors, resulting elliptical polarization

$$M_x = \frac{B_m}{2\Delta\kappa}\left(e^{j\omega t}(\kappa_{21} + j\kappa_{12}) + e^{-j\omega t}(\kappa_{22} - j\kappa_{12})\right) ,$$
$$M_y = -\frac{B_m}{2\Delta\kappa}\left(e^{j\omega t}(\kappa_{21} + j\kappa_{11}) + e^{-j\omega t}(\kappa_{21} - j\kappa_{12})\right) , \tag{10}$$
$$\mathbf{M} = M_x + jM_y .$$

The main and the off axes of the ellipses, 'a' and 'b', describing the components of the magnetization vector in *Fig. 2a-d* are determined by the elements of the anisotropy tensor, as

$$a_x = B_m\kappa_{22}/2\Delta\kappa, \quad b_x = B_m\kappa_{12}/2\Delta\kappa,$$
$$a_y = B_m\kappa_{11}/2\Delta\kappa, \quad b_y = B_m\kappa_{21}/2\Delta\kappa, \tag{11}$$

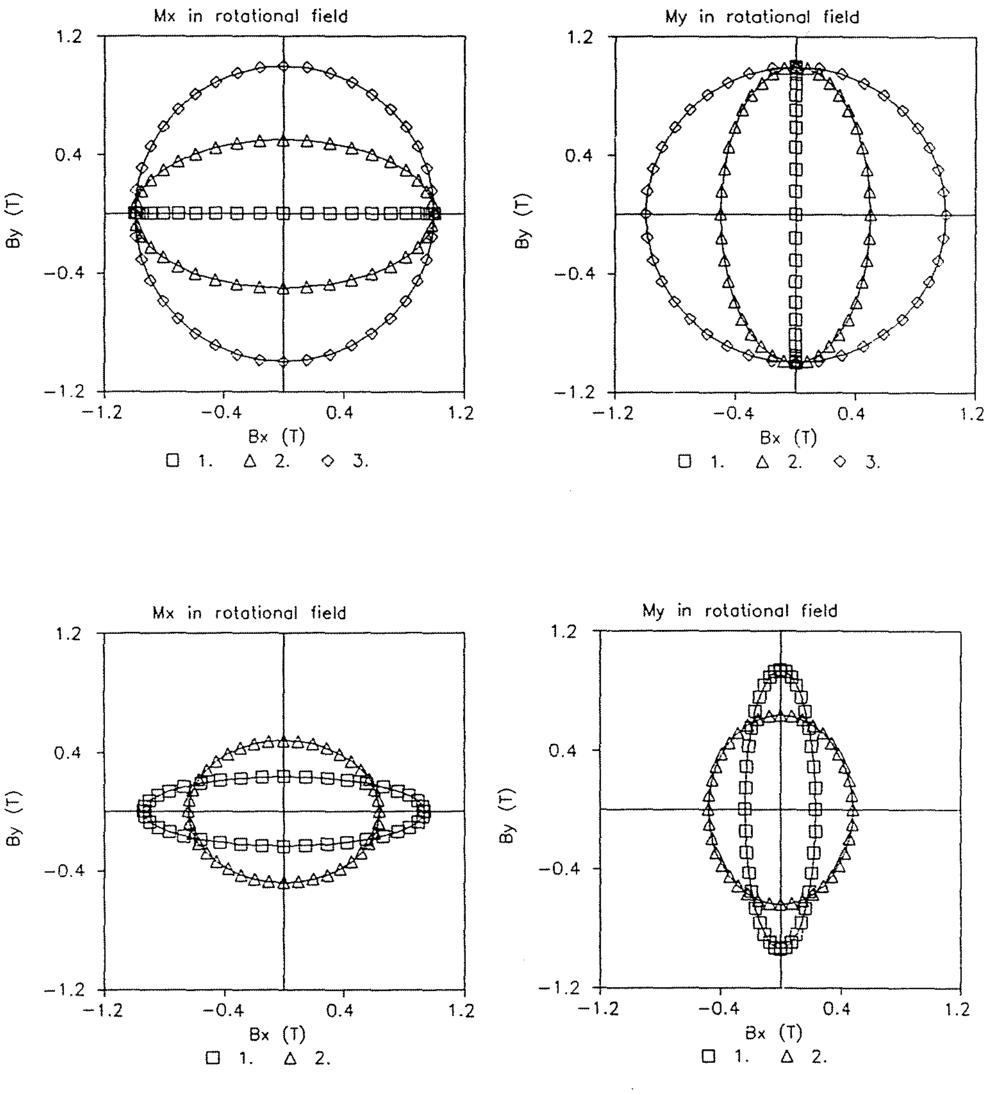

Fig. 2. Elliptical polarization in components of magnetization under rotational field at $B_m = 1$ T
(a) elliptical polarization in M_x at $\kappa_{11} = \kappa_{22} = 1.0$, $\kappa_{21} = 0.0$, curve 1. $\kappa_{12} = 0.0$, curve 2. $\kappa_{12} = 0.5$, curve 3. $\kappa_{12} = 1.0$
(b) elliptical polarization in M_y at $\kappa_{11} = \kappa_{22} = 1.0$, $\kappa_{12} = 0.0$, curve 1. $\kappa_{21} = 0.0$, curve 2. $\kappa_{21} = -0.5$, curve 3. $\kappa_{21} = -1.0$
(c) elliptical polarization in M_x at $\kappa_{11} = \kappa_{22} = 1.0$, curve 1. $\kappa_{12} = -\kappa_{21} = 0.25$, curve 2. $\kappa_{12} = -\kappa_{21} = 0.75$
(d) elliptical polarization in M_y at $\kappa_{11} = \kappa_{22} = 1.0$, curve 1. $\kappa_{12} = -\kappa_{21} = 0.25$, curve 2. $\kappa_{12} = -\kappa_{21} = 0.75$

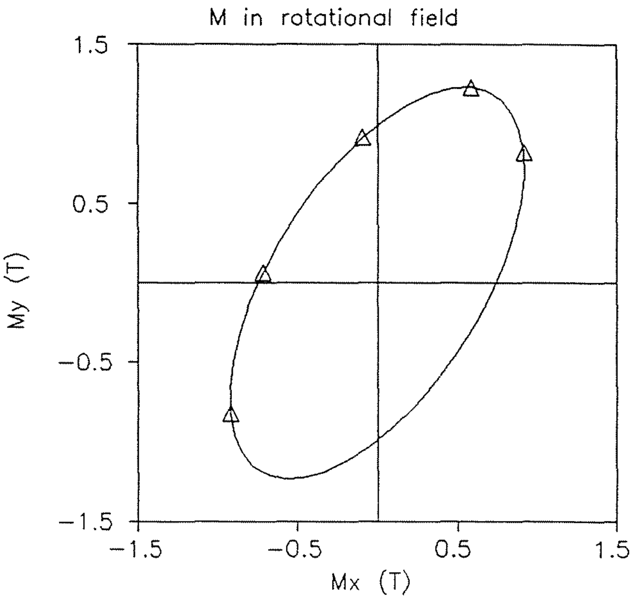

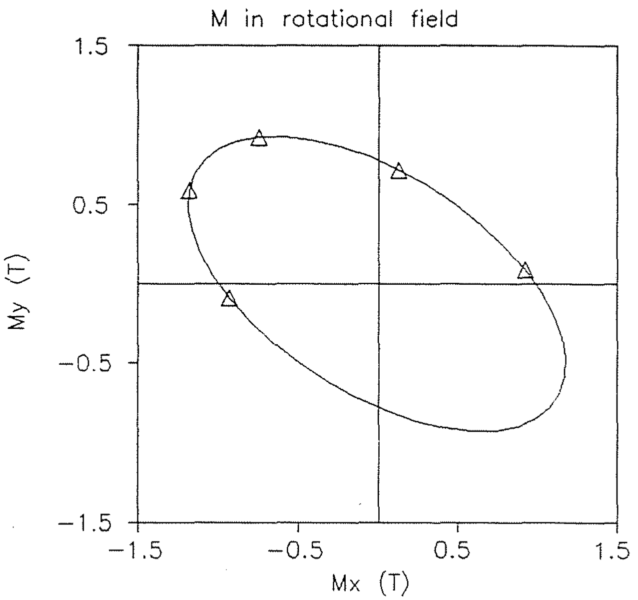

Fig. 3. Elliptical polarization in the magnetization under rotational field at $B_m = 1$ T
(a) elliptical polarization in M at $\kappa_{11} = \kappa_{22} = 1.0$, $\kappa_{12} = 0.1$, $\kappa_{21} = -0.8$
(b) elliptical polarization in M at $\kappa_{11} = \kappa_{22} = 1.0$, $\kappa_{12} = 0.8$, $\kappa_{21} = -0.1$

while for full polarization, plotted in *Fig. 3a-b*, the axes and the declination to the axis x can be determined as

$$
\begin{aligned}
a = {} & B_m(\sqrt{(\kappa_{22}+\kappa_{11})^2+(\kappa_{12}-\kappa_{21})^2}+ \\
& + \sqrt{(\kappa_{22}-\kappa_{11})^2+(\kappa_{12}+\kappa_{21})^2}))/2\Delta\kappa \ , \\
b = {} & B_m(\sqrt{(\kappa_{22}+\kappa_{11})^2+(\kappa_{12}-\kappa_{21})^2}+ \\
& + \sqrt{(\kappa_{22}-\kappa_{11})^2+(\kappa_{12}+\kappa_{21})^2}))/2\Delta\kappa \ , \\
\vartheta = {} & [\tan^{-1}((\kappa_{12}-\kappa_{21})/(\kappa_{11}+\kappa_{22}))+ \\
& + \tan^{-1}((\kappa_{12}+\kappa_{21})/(\kappa_{11}-\kappa_{22}))]/2 \ ,
\end{aligned}
\tag{12}
$$

where B_m is the amplitude of the applied flux density and $\Delta\kappa$ is the determinant of the tensor κ.

Selecting the main diagonal elements to be unit, in the anisotropy tensor the affection of the off-diagonal elements on the polarization is plotted in *Fig. 2* under the anti-clockwise rotating flux, $B_m = 1$ T. The polarization in the x, y directed components of the magnetization is plotted in *Fig. 2a* for $\kappa_{11} = \kappa_{22} = 1.0$, $\kappa_{21} = 0.0$ and $\kappa_{12} = 0.0$, 0.5, 1.0 parameters, while in *Fig. 2b* the parameters are elected as $\kappa_{11} = \kappa_{22} = 1.0$, $\kappa_{12} = 0.0$, $\kappa_{21} = 0.0$, -0.5, -1.0. To prove the affection of the off-diagonal elements the previous results are plotted for $\kappa_{11} = \kappa_{22} = 1.0$, at parameters $\kappa_{12} = -\kappa_{21} = 0.25$ and $\kappa_{12} = -\kappa_{21} = 0.75$ in *Fig. 2c-d*.

From *Fig. 2a-d* it can be seen that the main and the off-axes of the polarization in M_x and in M_y are determined by the elements of the anisotropy tensor.

The full polarization for the elements of the anisotropy tensor $\kappa = [1.0, 0.1, -0.8, 1.0]$ is plotted in *Fig. 3a* and for the value of anisotropy tensor $\kappa = [1.0, 0.8, -0.1, 1.0]$ in *Fig. 3b*.

From the plots it can be seen that the values of the main and off-axes do not change with the replacement in the off-diagonal elements. According to (12) the main and the off-axes in the polarization, plotted in *Fig. 3a* and in *Fig. 3b* are $a = 1.34$ T, $b = 0.69$ T, while the declinations to the x-axis are $\vartheta_a = 57.11°$ and $\vartheta_b = -32.89°$, resulting $\pi/2$ rotation in the main axis.

From the figures it can be seen that the interaction between the x, y components of the magnetic field yields different rate for polarization in the magnetization vector and in its components.

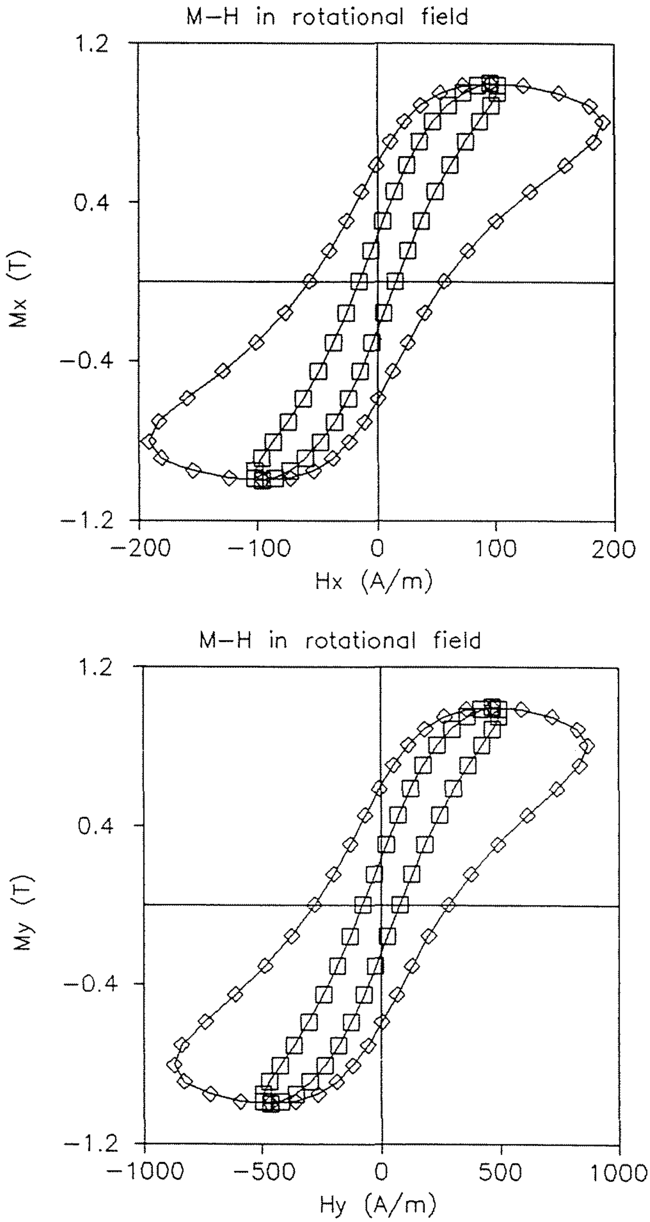

Fig. 4. The hysteresis loops generated by the anisotropy under rotational fields at $B_m =$ 1 T
(a) $M-H$ loop in x-direction at $\kappa_{11} = \kappa_{22} = 1.0$, $\kappa_{21} = 0.0$, curve 1. $\kappa_{12} = 0.25$, curve 2. $\kappa_{12} = 0.75$
(b) $M - H$ loop in y-direction at $\kappa_{11} = \kappa_{22} = 1.0$, $\kappa_{12} = 0.0$, curve 1. $\kappa_{21} = -0.25$, curve 2. $\kappa_{21} = -0.75$

3. Anisotropy and the Width of the Hysteresis

The other effect of the interaction between the flux components is the variation of the width of the hysteresis with the off-diagonal elements of the anisotropy tensor. Under $B_m = 1$ T anti-clockwise rotating flux the hysteresis loops generated by the anisotropy of the material are plotted in *Fig. 4a* for x-directed field components at $\kappa_{11} = \kappa_{22} = 1.0$, $\kappa_{21} = 0.0$ with $\kappa_{12} = 0.25$, 0.75 parameters and in *Fig. 4b* for y-directed components at $\kappa_{11} = \kappa_{22} = 1.0$, $\kappa_{12} = 0.0$, with $\kappa_{21} = -0.25$ -0.75 parameters.

From the figures it can be seen that the interaction between the x,y components of the magnetic field results magnetic hysteresis for the field components in the material characteristics.

Under $B_m = 1$ T rotational field the affection of the off-diagonal elements on the width of the hysteresis is examined. Selecting the main diagonal elements to be unit, over the $0 \leq \kappa_{12} \leq 1.0$, $-1.0 \leq \kappa_{21} \leq 0$ domain of the off-diagonal elements, the contour lines for the variation of the width in the hysteresis loops generated toward the x and the y directions are plotted in *Fig. 5a-b* and in *Fig. 5c-d*.

From the figures it can be seen that modelling the interaction in the rotational field with the off-diagonal elements of the anisotropy tensor, its variation modifies the width of the hysteresis.

To the further investigation for the material modelled after the measured samples [3] the main diagonal elements of the anisotropy tensor are selected to be unit, while the off-diagonal elements are determined from the width of the hysteresis loops. According to the measured data published in [3], the width of the hysteresis loop under $B_m = 0.5$ T rotational flux are $H_x = 30$ A/m, $H_y = 45$ A/m. To model the above material the selection for the elements of the anisotropy tensor $\kappa_{11} = \kappa_{22} = 1.00$, $\kappa_{12} = 0.95$, $\kappa_{21} = -0.30$ results near the same width in the hysteresis loops $H_x = 23.36$ A/m and $H_y = 35.48$ A/m under $B_m = 0.5$ T rotational flux.

4. Saturation Effect on the Polarization

To investigate what affection the amplitude of the rotating flux has on the **H**-field locus, first the variation of the width of the hysteresis with the amplitude of the applied flux is investigated.

At the above selection for the elements of the anisotropy tensor, the variation of the width fields in the hysteresis loops, H_x, H_y in the x and y directed hysteresis, versus the amplitude of the rotational flux is plotted in *Fig. 6*.

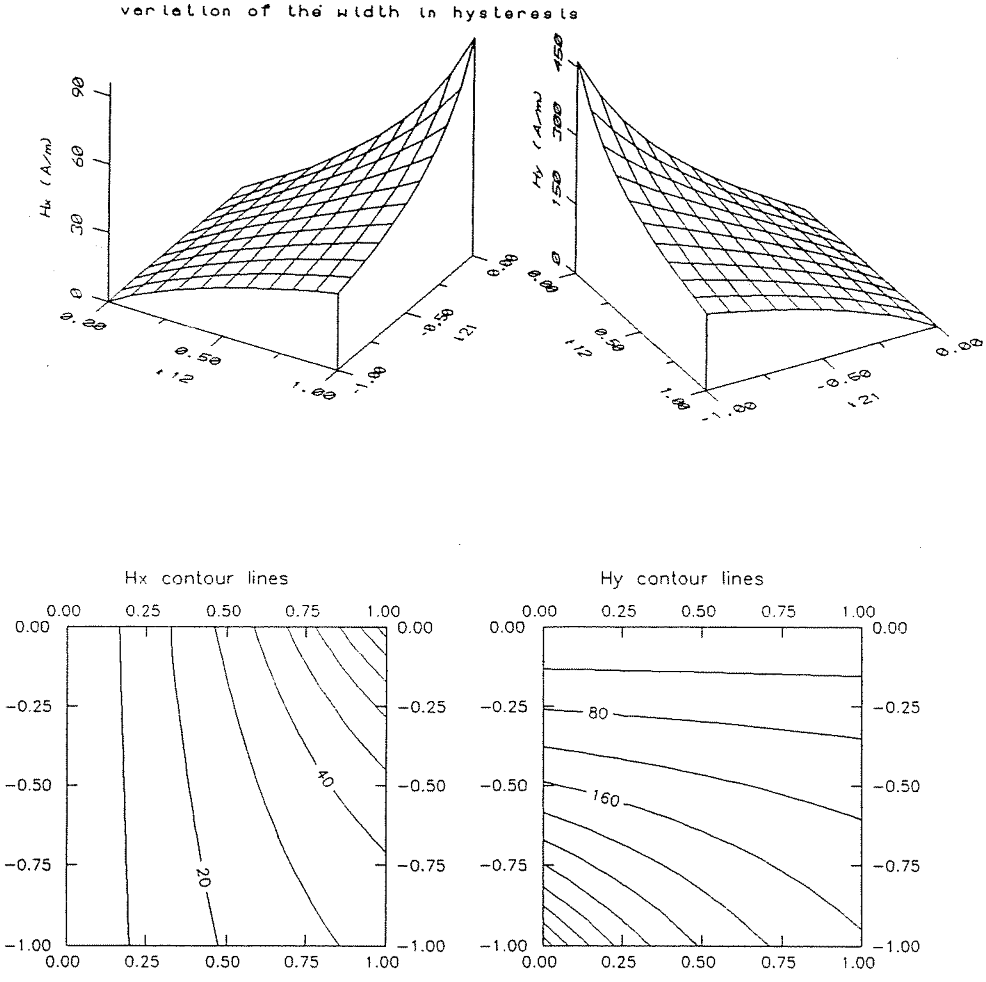

Fig. 5. Variation of the width of the hysteresis loops with the off-diagonal elements in the anisotropy tensor

(a) H_x field surface over the plane of the off-diagonal elements

(b) H_y field surface over the plane of the off-diagonal elements

(c) H_x field contour lines

(d) H_y field contour lines

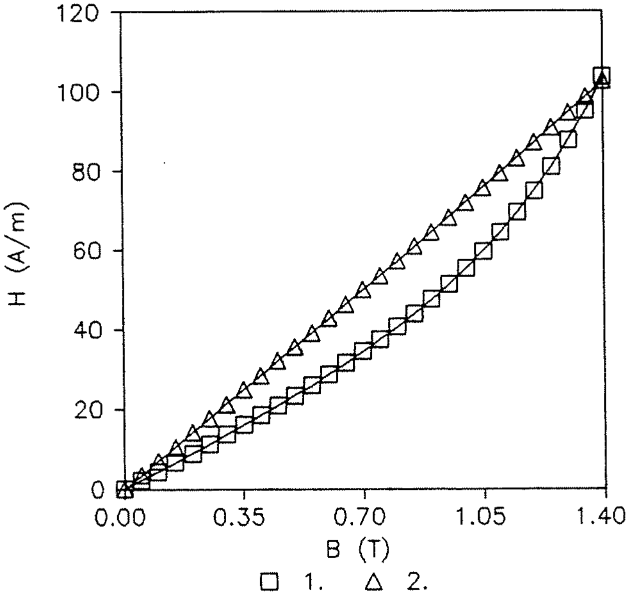

Fig. 6. Variation of the width of the hysteresis loops with the amplitude of the rotational flux density at $\kappa_{11} = \kappa_{22} = 1.0$, $\kappa_{12} = 0.95$, $\kappa_{21} = -0.3$, curve 1. $H_x = H(B_m)$, curve 2. $H_y = H(B_m)$

From the figures it can be seen that increasing either the values of the coefficients in the off-diagonal elements of the anisotropy tensor or the amplitude in the applied rotational field the width of the hysteresis loops toward different directions does not increase without limit. The other effect is that increasing the amplitude of the applied rotational field the width fields in the x and y directed hysteresis loops approximate the same value at saturation region.

Increasing the amplitude in the rotational flux, the modification of the hysteresis curves, and of the $\mathbf{H}$-field locus are plotted in *Fig. 7* at $B_m = 0.5$ T, in *Fig. 8* at $B_m = 1$ T, and in *Fig. 9* at $B_m = 1.3$ T under anti-clockwise rotating flux.

To explain the saturation effect, plotted in *Fig. 10* at $Bm = 1.4$ T, the nonlinear characteristics are approximated with 'broken lines' without hysteresis, and matching at the point given in (5) with the maximum value of the applied field

$$M_i = M_{oi} + \mu_i H_i \ ,$$

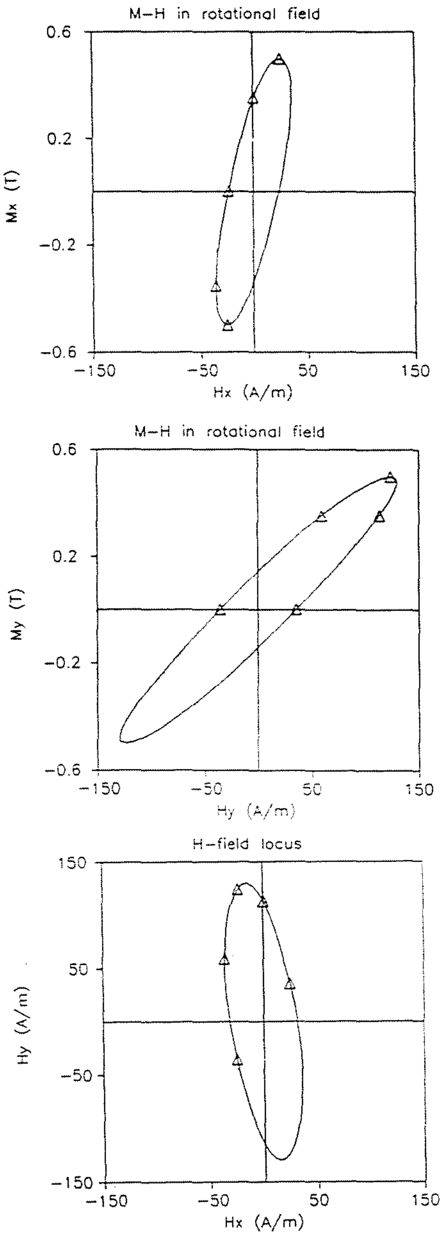

Fig. 7. Field patterns under rotational flux density $B_m = 0.5$ T
(a) hysteresis loop in x-direction
(b) hysteresis loop in y-direction
(c) $\mathbf{H}$-field locus

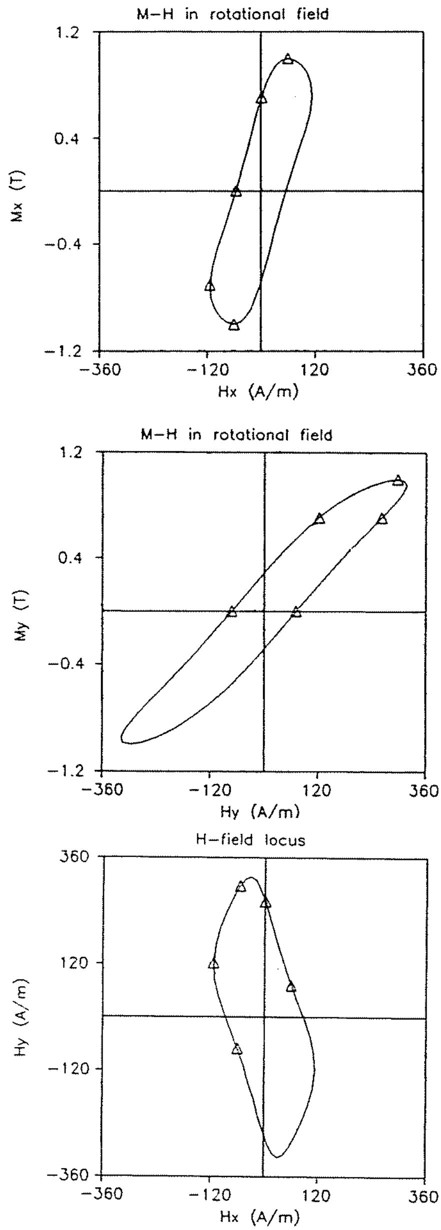

Fig. 8. Field patterns under rotational flux density $B_m = 1.0$ T
(a) hysteresis loop in x-direction
(b) hysteresis loop in y-direction
(c) $\mathbf{H}$-field locus

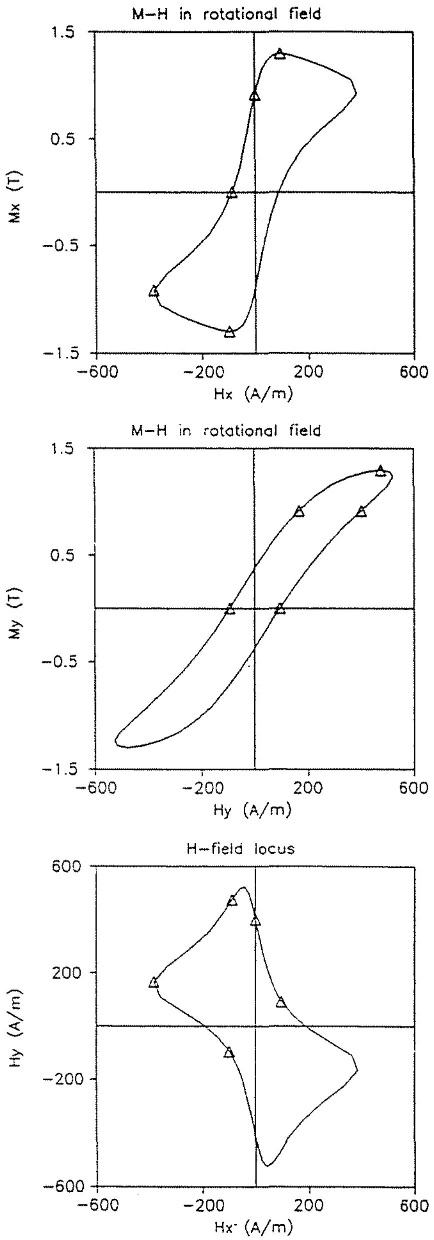

Fig. 9. Field patterns under rotational flux density $B_m = 1.3$ T
(a) hysteresis loop in x-direction
(b) hysteresis loop in y-direction
(c) $\mathbf{H}$-field locus

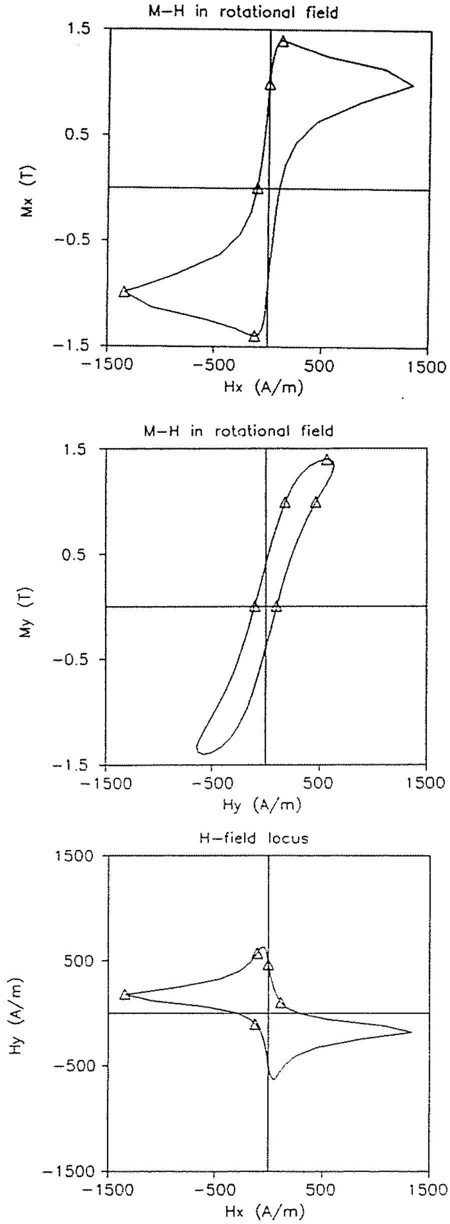

Fig. 10. Field patterns under rotational flux density $B_m = 1.4$ T
(a) hysteresis loop in x-direction
(b) hysteresis loop in y-direction
(c) **H**-field locus

$$M_i \begin{cases} = 0, & \mu_i = (dM_i/dH_i)|_{H_i=0}, \quad \text{for} \quad M_i \ll M_{m,i} \ , \\ \neq 0, & \mu_i = (dM_i/dH_i)|_{H_{m,i}}, \quad \text{for} \quad M_i \approx M_{m,i} \ , \end{cases} \quad i = x, y \ . \tag{13}$$

Substituting these characteristics into (3) the **H**-field locus can be reformulated as

$$H_x + jH_y = (M_x - M_{ox})/\mu_x + j(M_y - M_{oy})/\mu_y \ , \tag{14}$$

where M_x and M_y are responsible for the rotational flux, while μ_x, μ_y modify the elliptical polarization. If the amplitude of the rotational flux is far from the saturation value of the magnetization, so M_{ox},M_{oy} have zero values, and *Eq.* (14) yields elliptical polarized form for the **H**-field locus.

If a saturation is supposed in the x-directed **H**-field, the y-directed field, is far from the saturation according to the phase shift between the x, y components of the flux, and in spite of the interaction. So, the first term in (14) results the saturation value for H_x, while the second term results a polarization with small amplitude. Repeating the same process in y-direction, it results in the saturated value of y-components of H-field with small amplitude of polarization [4]. The phase position of these extreme fields can be determined from (13). If there is large difference between the saturation values of different directions, and the x, y components of the flux have $\pi/2$ phase shift, the extreme values in **H**-field locus are near to the axes of the field components as it can be seen in *Fig. 10.*

Conclusion

Feeding a nonlinear material with rotational flux its characteristics prove different properties comparing to the one under alternating flux.

The rotational flux results hysteresis for anisotropic material, having anhysteretic characteristic in alternating field.

In the material which under rotational flux does not reach the saturation region of the characteristics, the **H**-field locus follows the elliptical polarization of the magnetization patterns. Under rotational flux the saturation effect in any direction yields a strong displacement in the **H**-field patterns resulting modification in the field locus.

References

1. IVÁNYI, A.: Energy in Oriented Lamination, *International Journal of Applied Electromagnetics*, Vol. 4. 1993. pp. 137–143.
2. ENOKIZONO, M.: Constitutive Equations $\mathbf{B} = \mu\mathbf{H}$ and Two-dimensional Magnetic Properties, *Proceedings of the Second International Workshop on Two-Dimensional*

Magnetic Measurement and its Properties, 31. Jan. – 1. Febr. 1992. Oita, Japan, JSAEM Studies in Applied Electromagnetics, Vol. 1. pp. 3–16.

3. TANAKA, T. – TAKADA, S. – SASAKI, T.: Measurement of AC Magnetic Properties in a Single Strip Sample, *Proceedings of the Second International Workshop on Two-Dimensional Magnetic Measurement and its Properties*, 31. Jan. – 1. Febr. 1992. Oita, Japan, JSAEM Studies in Applied Electromagnetics, Vol. 1. pp. 43–55.
4. MOSES, A. J. – MEYDAN, T.: Results of Thermal and H-coil Sensor Measurements of Rotational Loss in Soft Magnetic Materials, *Proceedings of the Second International Workshop on Two-Dimensional Magnetic Measurement and its Properties*, 31. Jan. – 1. Febr. 1992. Oita, Japan, JSAEM Studies in Applied Electromagnetics, Vol. 1. pp. 71–82.